

Higher-multipole deformations and compactness of hot fusion reactionsMonika Manhas,^{1,2} Raj K. Gupta,^{1,2} Qingfeng Li,² S. K. Patra,^{2,3} and Walter Greiner²¹*Department of Physics, Panjab University, Chandigarh 160014, India*²*Frankfurt Institute for Advanced Studies (FIAS), Johann Wolfgang Goethe-Universität, Max-von-Laue-Str. 1, D-60438 Frankfurt am Main, Germany*³*Institute of Physics, Sachivalaya Marg, Bhubaneswar 751005, India*

(Received 12 June 2006; published 15 September 2006)

The effect of adding the higher-multipole deformations β_6 and β_8 , and the octupole deformation β_3 (in addition to quadrupole and hexadecapole deformations β_2 and β_4), on the distribution of barriers in orientation degrees of freedom is studied for a “compact” configuration of spherical-plus-deformed or deformed-plus-deformed nuclei in hot fusion reactions. Though β_3 is known to be nonzero for only a few nuclei, its role toward compactness of hot fusion reactions is found to be as important as that of β_4 . With β_3 included, depending on its sign and magnitude, the belly-to-belly compact, bbc (or equatorial compact, ec), configuration due to β_4 changes to not-belly-to-belly compact, nbbc (or not-equatorial compact, nec), and vice versa. Similarly, β_6 is found to be as important as β_3 and/or β_4 for spherical-plus-deformed nuclei, but is rather insignificant for collisions involving deformed-plus-deformed nuclei. On the other hand, the addition of β_8 is shown to be insignificant also for spherical-plus-deformed nuclei.

DOI: [10.1103/PhysRevC.74.034603](https://doi.org/10.1103/PhysRevC.74.034603)

PACS number(s): 24.10.–i

I. INTRODUCTION

Experimentally, the compactness of hot fusion reactions is observed recently in the measured excitation functions for the 4n channels in $^{48}\text{Ca}+^{242,244}\text{Pu}\rightarrow^{290,292}114^*$ reactions [1,2] and for the 3n channel in the $^{48}\text{Ca}+^{238}\text{U}\rightarrow^{286}112^*$ reaction [2]. It is noticed that, compared to the well-studied $^{206,208}\text{Pb}$ -based cold fusion reactions with excitation energies of $E^* \sim 10$ –20 MeV, the peaks of the excitation functions in these ^{48}Ca -based reactions are broader as well as shifted to higher $E^* \sim 35$ –41 MeV, which could arise if the collisions correspond to more compact configurations of the type of equator-cross (here “equatorial” (e), as one of the nuclei is spherical) or belly-to-belly for collisions in the same plane (azimuthal angle $\phi = 0^\circ$) since the barriers are then higher by about 20 MeV, compared to the “elongated” pole-to-pole (“polar” for deformed + spherical cases) collisions. A higher barrier means an increased fusion threshold or an increased number of emitted neutrons. Theoretically, for a hot fusion reaction, the barrier is highest and the interaction radius smallest [3], which for a “compact” reaction occurs for collisions in the directions of the minor axes of the (deformed) reaction partners, i.e., for their $90^\circ, 90^\circ$ orientations, the belly-to-belly or equator-cross configuration [4]. If one of the nuclei is spherical, we get an “equatorial compact” (ec) configuration, the 90° orientation of the deformed reaction partner.

In a recent article [5], based on generalized fragmentation theory which includes the orientation degrees of freedom and higher multipole deformations within the nuclear proximity potential [6,7], some of us have shown that the magnitudes of both the quadrupole (β_2) and the hexadecapole (β_4) deformations of the reaction partners play an important role in the distribution of barriers in orientation degrees of freedom. It is shown that a belly-to-belly compact (bbc) (equatorial compact, ec, if one of the reaction partners is spherical) configuration is obtained if the nuclei have the quadrupole deformations alone

or are with additional small (including negative) hexadecapole deformations. Yet, the presence of large (positive) hexadecapole deformation results in a not-belly-to-belly compact (nbbc) or not-equatorial compact (nec) configuration. For the compactness of the ^{48}Ca -induced reactions, it is shown that the reactions leading to $Z \geq 114$ compound systems are the “compact hot fusion” reactions at an ec (orientation angle $\theta = 90^\circ$) configuration, but the ones for $Z < 114$ systems are compact at a nec ($\theta < 90^\circ$) configuration. The two compact configurations (ec and nec) differ by as much as 22° .

The magnitudes of other higher-multipole deformations ($\beta_6, \beta_8 \dots$) should, however, also be important for the distribution of barriers in orientation degrees of freedom, i.e., for the angle(s) of orientation giving the most compact configuration. This aspect of the problem for collisions between deformed nuclei has not been investigated at all and is studied here in this article for the first time. Also, the role of including the octupole deformation (β_3) is investigated here in some more detail, though β_3 is, in general, zero. We find that the sign of β_3 , wherever available [8], is negative and its inclusion always favors an ec configuration. On the other hand, β_6 has both the positive and negative signs [8], and both its sign and magnitude play an important role in choosing an ec or a nec configuration. The β_8 deformations are not available in Ref. [8], but are given in another study [9]. Since both the signs and the magnitudes of given deformations in these two studies differ greatly, we choose β_8 values arbitrarily and consider both its positive and negative signs. The sign of β_8 is negative in Ref. [9]. The relevant questions to be answered are: (i) how important is it to include β_3 , wherever available, and (ii) do the higher-order deformations (β_6, β_8 , etc.) reinforce the result of lower order (β_3 and β_4) contributions to quadrupole deformation or do they cancel each other out to, effectively, leave the quadrupole deformation β_2 alone? The result of our present investigation is that addition of β_3 is as important

as that of β_4 and that, depending on the sign(s), the β_6 deformations reinforce the result of lower-order deformations, the important ones being thus β_2, β_3 , and β_4 mainly. For example, for spherical-plus-deformed nuclei and with $\beta_3 = 0$, the addition of β_6 behaves inverse of β_4 ; i.e., positive β_6 favors an ec configuration whereas negative (and small positive) β_6 favors a nec configuration. Moreover, for deformed + deformed collisions, independent of its sign, the role of β_6 is simply to reinforce the result of β_4 or $\beta_3 + \beta_4$. Similarly, β_8 also reinforces the above result, for both the spherical-plus-deformed and the deformed-plus-deformed collisions. We use here the generalized fragmentation theory [3–5] for our study.

This article is organized as follows. Section II gives briefly the theoretical formalism used and Sec. III gives the results of our calculations. Finally, a summary of our results is presented in Sec. IV.

II. THE GENERALIZED FRAGMENTATION THEORY FOR DEFORMED AND ORIENTED NUCLEI

Using the coordinates of mass and charge asymmetries $\eta = (A_1 - A_2)/(A_1 + A_2)$ and $\eta_Z = (Z_1 - Z_2)/(Z_1 + Z_2)$; the relative separation \bar{R} ; the deformations $\beta_{\lambda i}$, $\lambda = 2, 3, 4, 6$, and 8 ; the quadrupole, octupole, hexadecapole deformations, etc., of two nuclei ($i = 1, 2$); the two orientation angles θ_i ; and the azimuthal angle ϕ between the principal planes of two nuclei, the scattering potential in the generalized fragmentation theory for the fixed η and η_Z values is given by

$$V(R)|_{\eta, \eta_Z} = V_C(R, Z_i, \beta_{\lambda i}, \theta_i, \phi) + V_P(R, A_i, \beta_{\lambda i}, \theta_i, \phi). \quad (1)$$

$\phi = 0^\circ$ for coplanar nuclei, and only one orientation angle θ is enough for spherical-plus-deformed collisions, referring to the rotationally symmetric deformed nucleus. V_C and V_P are, respectively, the Coulomb and nuclear proximity potentials for the $\phi = 0^\circ$ case, given by

$$V_C = \frac{Z_1 Z_2 e^2}{R} + 3Z_1 Z_2 e^2 \sum_{\lambda, i=1,2} \frac{1}{2\lambda+1} \frac{R_i^\lambda(\alpha_i)}{R^{\lambda+1}} Y_\lambda^{(0)}(\theta_i) \times \left[\beta_{\lambda i} + \frac{4}{7} \beta_{\lambda i}^2 Y_\lambda^{(0)}(\theta_i) \right] \quad (2)$$

and

$$V_P = 4\pi \bar{R} \gamma b \Phi(s_0), \quad (3)$$

where, for the axially symmetric shapes,

$$R_i(\alpha_i) = R_{0i} \left[1 + \sum_{\lambda} \beta_{\lambda i} Y_\lambda^{(0)}(\alpha_i) \right], \quad (4)$$

with $R_{0i} = 1.28A_i^{1/3} - 0.76 + 0.8A_i^{-1/3}$, the specific surface energy constant $\gamma = 0.9517 [1 - 1.7826 \{(N - Z)/A\}^2]$ (in MeV fm⁻²), the nuclear surface thickness $b = 0.99$ fm, and the universal function $\Phi(s_0)$, which depends only on the minimum separation distance s_0 , is

$$\Phi(s_0) = \begin{cases} -\frac{1}{2}(s_0 - 2.54)^2 - 0.0852(s_0 - 2.54)^3, \\ -3.437 \exp\left(-\frac{s_0}{0.75}\right) \end{cases} \quad (5)$$

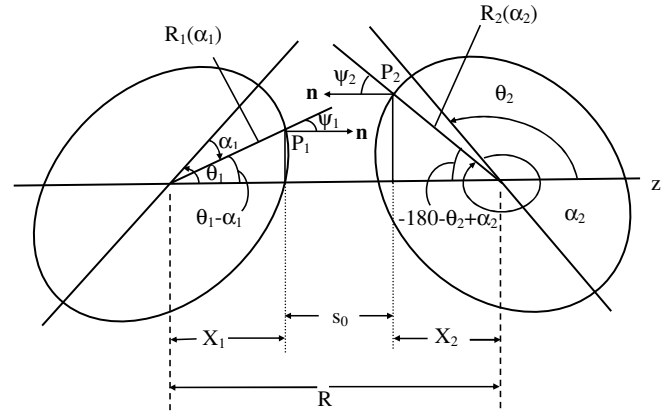


FIG. 1. Schematic configuration of any two axially symmetric deformed, oriented nuclei lying in the same plane ($\phi = 0^\circ$).

respectively, for $s_0 \leq 1.2511$ and ≥ 1.2511 . The minimized separation distance s_0 , in units of b , for coplanar nuclei is defined [6] as (see Fig. 1)

$$s_0 = R - X_1 - X_2 = R - R_1(\alpha_1) \cos(\theta_1 - \alpha_1) - R_2(\alpha_2) \cos(180 + \theta_2 - \alpha_2), \quad (6)$$

with the minimization conditions (in α_i)

$$\begin{aligned} \tan(\theta_1 - \alpha_1) &= -\frac{R'_1(\alpha_1)}{R_1(\alpha_1)} \\ \tan(180 + \theta_2 - \alpha_2) &= -\frac{R'_2(\alpha_2)}{R_2(\alpha_2)}. \end{aligned} \quad (7)$$

Here, $R'_i(\alpha_i)$ are the first-order derivatives of $R_i(\alpha_i)$ with respect to α_i . The mean curvature radius \bar{R} , characterizing s_0 , i.e., the points of closest approach for nuclei lying in the same plane ($\phi = 0^\circ$), is

$$\frac{1}{\bar{R}^2} = \frac{1}{R_{11}R_{12}} + \frac{1}{R_{21}R_{22}} + \frac{1}{R_{11}R_{22}} + \frac{1}{R_{21}R_{12}}, \quad (8)$$

with R_{i1} and R_{i2} as the principal radii of curvatures at the two points of closest approach of nuclei. For explicit expressions of R_{i1} and R_{i2} and other details, we refer the reader to [6]. We use the same formalism as above for noncoplanar nuclei ($\phi \neq 0^\circ$), but do not address these considerations in this article because only the $\phi = 0^\circ$ case is studied. The details of the non-coplanar $\phi \neq 0^\circ$ case can be seen in Ref. [7].

III. CALCULATIONS AND RESULTS

First, we study the effect of adding the octupole deformation β_3 on the angle of compactness θ_c . We choose the reaction $^{226}\text{Ra} + ^{54}\text{Ti} \rightarrow ^{280}\text{Ds}^*$, where ^{226}Ra is the deformed reaction partner having the deformations β_2, β_3 , and β_4 . ^{54}Ti is a spherical nucleus. We know from our earlier study [5] that this is a nec reaction if only β_2 and β_4 deformations are allowed (a case of large, positive β_4), as is depicted in Fig. 2 (dashed line) where the barrier height V_B is plotted as a function of the orientation angle θ . On the other hand, if β_3 is added (solid

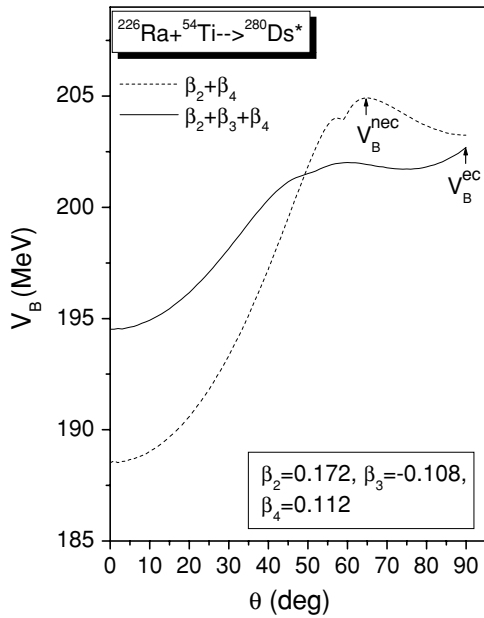


FIG. 2. The barrier height V_B plotted as a function of the orientation angle θ of the deformed nucleus ^{226}Ra for the reaction $^{226}\text{Ra}+^{54}\text{Ti}\rightarrow^{280}\text{Ds}^*$. The higher-order deformations β_3 and β_4 are included, and angle θ is varied in a small step of 1° . The maximum barrier-heights V_B^{ec} and V_B^{nec} , pointing out to the most compact configurations at $\theta = 90^\circ$ (equatorial compact, ec) and $\theta < 90^\circ$ (not-equatorial compact, nec), respectively, are also marked.

line), it is evident from Fig. 2 that the highest barrier is shifted to $\theta_c = 90^\circ$, the ec configuration. Note that here β_3 has a large, negative value.

Next, to see the role of the magnitude of β_3 , we plot in Fig. 3, for the same reaction as above, the barrier heights V_B and positions R_B as functions of the deformation β_3 , calculated for different orientation angles θ , varying β_3 from -0.11 to $+0.05$, a maximum available negative [8] to some arbitrary positive value. We notice in this figure that an ec configuration ($\theta_c = 90^\circ$; highest V_B or smallest R_B) is obtained for all large, negative β_3 values, but goes over to nec for all positive and very small negative (including zero) β_3 values. Interestingly, if we have an ec reaction, such as the $^{244}\text{Pu}+^{48}\text{Ca}\rightarrow^{292}114^*$ reaction in Fig. 4(a), where β_4 is small positive (the same would be true for a case with any negative β_4 value) it remains ec for all negative β_3 values (including zero) and becomes nec for all positive β_3 values. Furthermore, we get the same result as in Fig. 3 if we replace the spherical ^{54}Ti by a deformed ^{60}Cr nucleus. This is depicted in Fig. 4(b), a case of nbcc reaction since the β_{41} value is large positive and $\beta_{32} = 0$. Thus, depending on the magnitude of β_{41} (β_4 if the other nucleus is spherical), the addition of β_{31} (β_3 for the other nucleus to be spherical) results in a bbc configuration for negative β_{31} values and a nbcc configuration for positive β_{31} values. In other words, for cases of large positive β_{41} (the nbcc configurations), only large negative β_{31} values give rise to bbc configurations; the small negative β_{31} values behave as the zero or

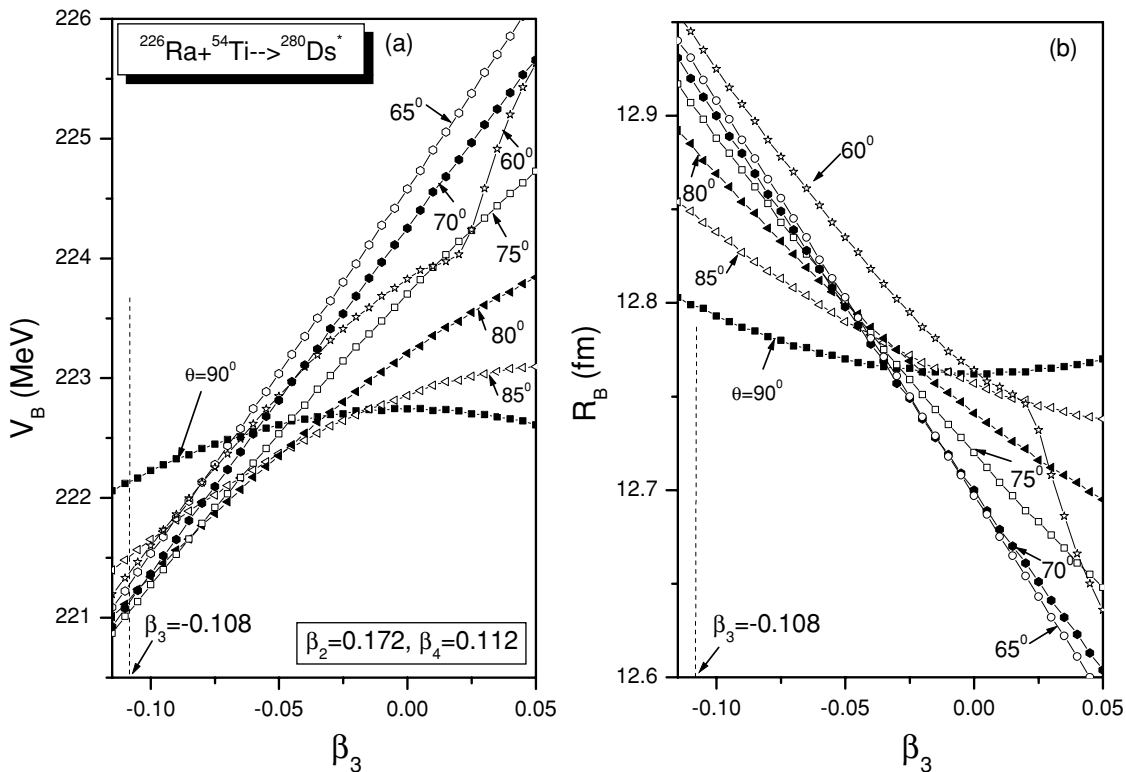


FIG. 3. The barrier height V_B and barrier position R_B as a function of the octupole deformation parameter β_3 , for different orientation angles θ , calculated for the reaction $^{226}\text{Ra}+^{54}\text{Ti}\rightarrow^{280}\text{Ds}^*$. The β_3 value of ^{226}Ra is also marked.

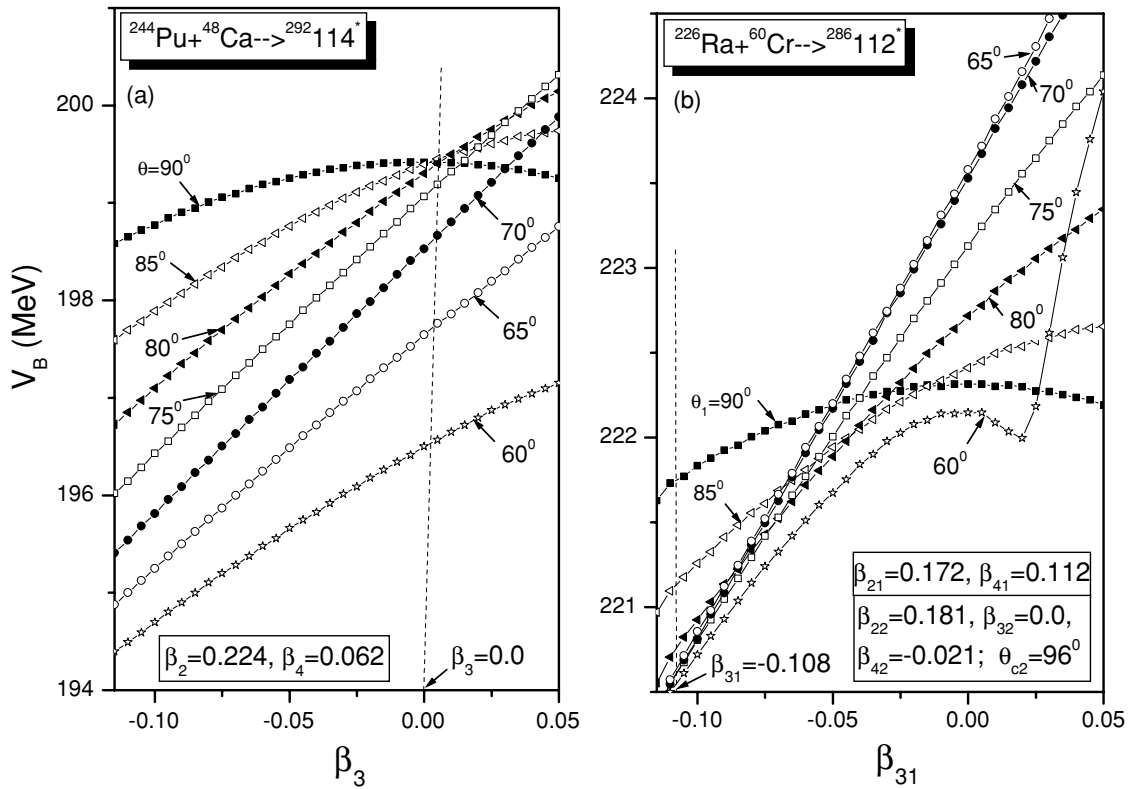


FIG. 4. The same as for Fig. 3, but for barrier height V_B alone, and for the reactions $^{244}\text{Pu} + ^{48}\text{Ca} \rightarrow ^{292}114^*$ and $^{226}\text{Ra} + ^{60}\text{Cr} \rightarrow ^{286}112^*$. Note that ^{60}Cr is also deformed and has the compact orientation $\theta_{c2} = 96^\circ$ [5]. The values of β_3 and β_{31} , respectively, for ^{244}Pu and ^{226}Ra are also marked.

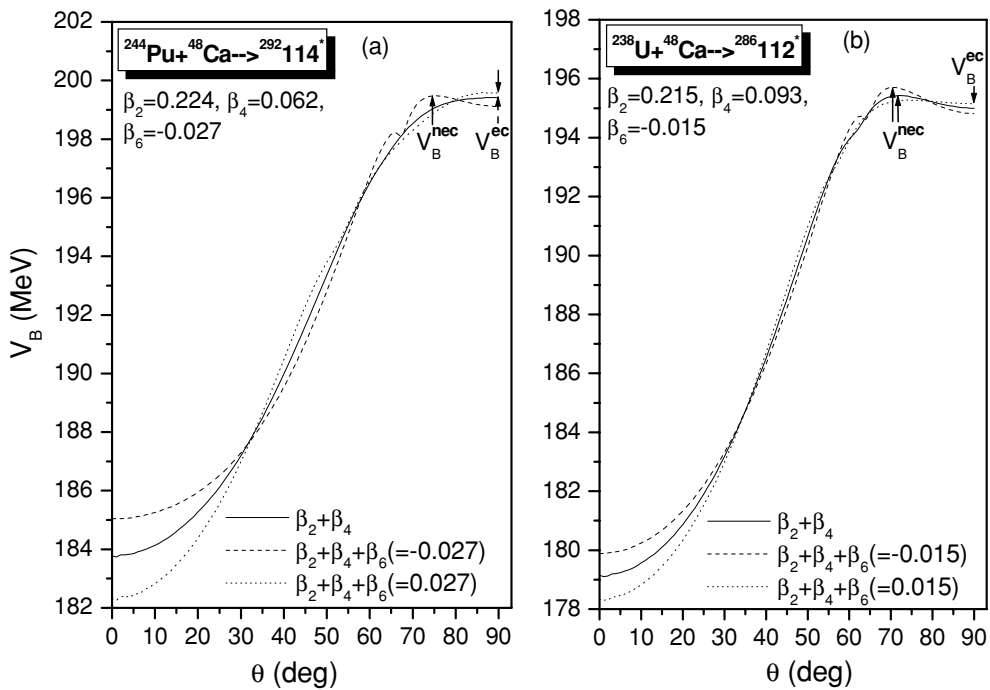


FIG. 5. The same as for Fig. 2, but for the reactions $^{244}\text{Pu} + ^{48}\text{Ca} \rightarrow ^{292}114^*$ and $^{238}\text{U} + ^{48}\text{Ca} \rightarrow ^{286}112^*$. The higher-order deformations β_4 and β_6 are included, and both the positive and negative signs of β_6 are considered.

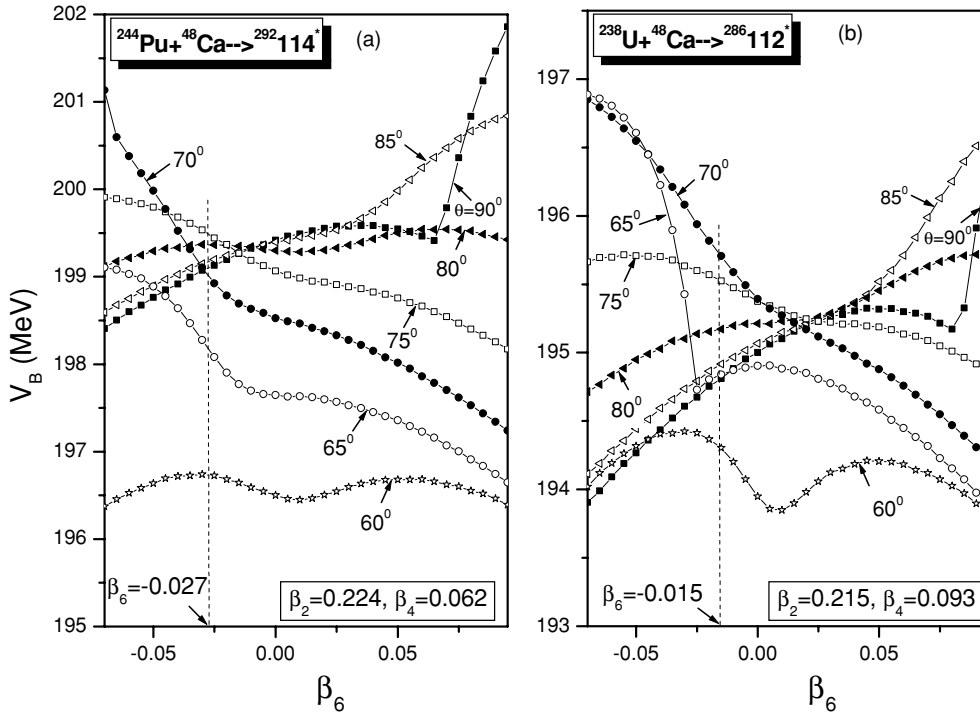


FIG. 6. The barrier height V_B as a function of the deformation parameter β_6 , for different orientation angles θ , calculated for the reactions $^{244}\text{Pu}+^{48}\text{Ca}\rightarrow^{292}114^*$ and $^{238}\text{U}+^{48}\text{Ca}\rightarrow^{286}112^*$. The β_6 values of deformed partners are also marked. Note that here $\beta_3 = 0$ for both the reactions.

positive β_{31} values such that the nbcc configuration remains nbcc. Hence, the relative magnitudes of both the β_{31} and β_{41} (or β_3 and β_4 if the other nucleus is spherical) deformations play the decisive role in the distribution of barriers in orientation degrees of freedom, i.e., for fixing the orientation angle(s) θ_{ci} (or θ_c) of the most compact configuration.

Figure 5(a) shows the effects of adding the β_6 deformation on the compact orientation of the reaction $^{244}\text{Pu}+^{48}\text{Ca}\rightarrow^{292}114^*$. This is a case of $\beta_3 = 0$ and with small positive β_4 , and hence an ec reaction for $\beta_2 + \beta_4$ deformations alone (the same would be true for a case of any negative β_4 added to β_2). We notice that inclusion of negative β_6 changes the ec to a nec configuration, whereas the same with positive β_6 leaves it unchanged, i.e., ec remains as ec. A reverse of this situation is presented in Fig. 5(b) for the case of large positive β_4 , nec reaction $^{238}\text{U}+^{48}\text{Ca}\rightarrow^{286}112^*$; i.e., negative β_6 leaves the nec unchanged as nec and positive β_6 changes nec to ec. Thus, the addition of β_6 seems to reinforce the result obtained for β_4 , but with opposite sign; i.e., the large negative β_6 when added to large positive β_4 results in a nec configuration and vice-versa for the ec configuration. The same result is evident from Fig. 6 where both the cases of small and large β_4 values are considered and β_6 is varied from -0.075 to 0.095 , the limiting values from Ref. [8]. For the case of small β_4 [Fig. 6(a)], the ec (or near-ec) configuration remains the same for positive β_6 and becomes the nec configuration for negative β_6 , whereas an inverse of the above result is true for the case of the large β_4 in Fig. 6(b); i.e., the nec configurations remains nec for negative β_6 and becomes the ec (or near-ec)

configuration for positive β_6 . Interestingly, the same result also holds good for β_6 added to the case of $\beta_2 + \beta_4$ plus (negative) β_3 deformations. This calculation is presented in Fig. 7 for the case of an ec configuration due to $\beta_2 + \beta_3 + \beta_4$, though it is a case of large positive β_4 . Figure 7 presents almost the same result as shown in Fig. 6(a), the two being the cases of

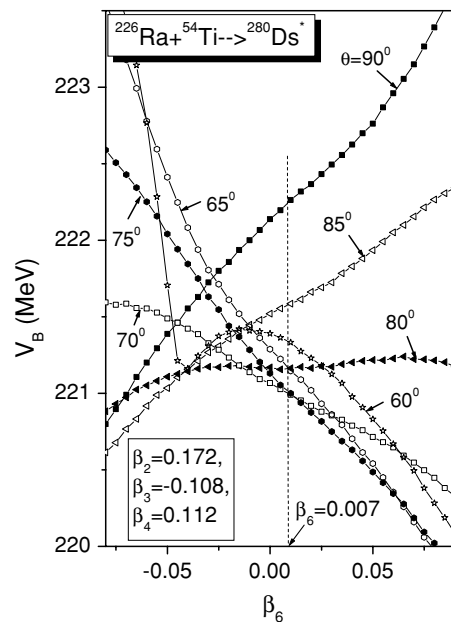


FIG. 7. The same as for Fig. 6 but for the reaction $^{226}\text{Ra}+^{54}\text{Ti}\rightarrow^{280}\text{Ds}^*$ with nonzero β_3 value for the deformed partner.

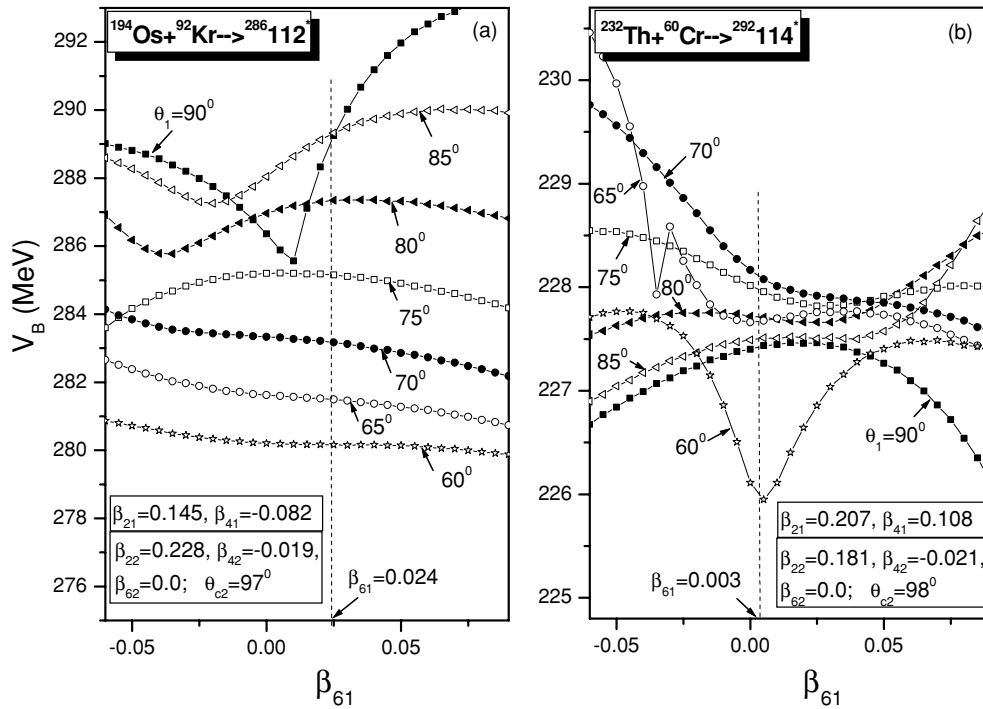


FIG. 8. The same as for Fig. 4, but for the reactions $^{194}\text{Os}+^{92}\text{Kr}\rightarrow^{286}112^*$ and $^{232}\text{Th}+^{60}\text{Cr}\rightarrow^{292}114^*$. Both ^{92}Kr and ^{60}Cr are deformed, respectively, with compact orientations $\theta_{c,2} = 97^\circ$ and 98° [5]. The values of β_{61} for ^{194}Os and ^{232}Th are also marked.

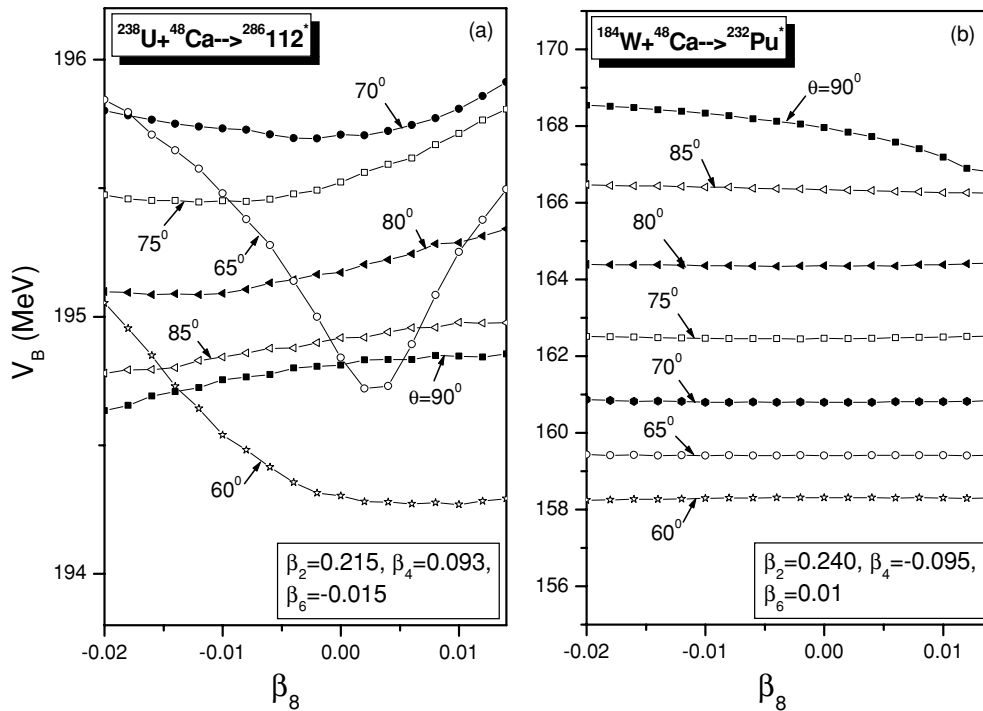


FIG. 9. The same as for Fig. 8, but as a function of the deformation parameter β_8 and for the reactions $^{238}\text{U}+^{48}\text{Ca}\rightarrow^{286}112^*$ and $^{184}\text{W}+^{48}\text{Ca}\rightarrow^{232}\text{Pu}^*$. The reactions are so chosen that the combined effect of their β_4 and β_6 result in nec and ec reactions, respectively.

TABLE I. Magnitudes and signs of higher-multipole deformations added to quadrupole deformation for compact configurations.

ec configuration	nec configuration
$\beta_2 + \beta_4$	$\beta_2 + \beta_4$
$0 <^a \beta_4 \leq 0$	$\beta_4 \gg 0$
$\beta_2 + \beta_3 + \beta_4$	$\beta_2 + \beta_3 + \beta_4$
$0 <^a \beta_4 \leq 0$ with $\beta_3 \leq 0$	$\beta_4 \gg 0$ with $0 >^b \beta_3 \geq 0$
If $\beta_4 \gg 0$, then $\beta_3 \ll 0$	If $0 <^a \beta_4 \leq 0$, then $\beta_3 > 0$
$\beta_2 + \beta_4 + \beta_6$ ($\beta_3 = 0$)	$\beta_2 + \beta_4 + \beta_6$ ($\beta_3 = 0$)
$0 <^a \beta_4 \leq 0$ with $\beta_6 > 0$	$\beta_4 \gg 0$ with $0 <^a \beta_6 \leq 0$
If $\beta_4 \gg 0$, then $\beta_6 \gg 0$	If $0 <^a \beta_4 \leq 0$, then $\beta_6 < 0$
$\beta_2 + \beta_3 + \beta_4 + \beta_6$ ($\beta_3 \neq 0$)	$\beta_2 + \beta_3 + \beta_4 + \beta_6$ ($\beta_3 \neq 0$)
$\beta_3 < 0$ with $0 \leq \beta_6 <^b 0$	$\beta_3 < 0$ with $\beta_6 \ll 0$
	$\beta_3 > 0$ with $0 < \beta_6 < 0$
$\beta_2 + \beta_3 + \beta_4 + \beta_6 + \beta_8$	$\beta_2 + \beta_3 + \beta_4 + \beta_6 + \beta_8$
$0 < \beta_8 < 0$	$0 < \beta_8 < 0$
bbc or near-bbc ^c configuration	nbbc configuration
$\beta_{2i} + \beta_{4i}$ ($i = 1, 2$)	$\beta_{2i} + \beta_{4i}$
$0 <^a \beta_{4i} \leq 0$	$\beta_{4i} \gg 0$
$\beta_{2i} + \beta_{3i} + \beta_{4i}$	$\beta_{2i} + \beta_{3i} + \beta_{4i}$
$0 <^a \beta_{4i} \leq 0$ with $\beta_{3i} \leq 0$	$\beta_{4i} \gg 0$ with $0 >^b \beta_{3i} \geq 0$
If $\beta_{4i} \gg 0$, then $\beta_{3i} \ll 0$	If $0 <^a \beta_{4i} \leq 0$, then $\beta_{3i} > 0$
$\beta_{2i} + \beta_{3i} + \beta_{4i} + \beta_{6i}$	$\beta_{2i} + \beta_{3i} + \beta_{4i} + \beta_{6i}$
$0 < \beta_{6i} < 0$	$0 < \beta_{6i} < 0$
$\beta_{2i} + \beta_{3i} + \beta_{4i} + \beta_{6i} + \beta_{8i}$	$\beta_{2i} + \beta_{3i} + \beta_{4i} + \beta_{6i} + \beta_{8i}$
$0 < \beta_{8i} < 0$	$0 < \beta_{8i} < 0$

^aSmall positive.^bSmall negative.^cNear-bbc means bbc within approximately $\pm 5^\circ$.

ec configuration when $\beta_6 = 0$. On the other hand, if $\beta_3 > 0$, we get the nec configuration for all (positive and negative) β_6 values (not shown here). Furthermore, for the case of the two deformed nuclei in Fig. 8, we notice that the addition of β_{61} leaves the compact configurations unchanged; i.e., the bbc or near-bbc, for the case of negative β_{41} , remains bbc or near-bbc and the nbbc, for the case of large positive β_{41} , remain nbbc. In other words, for the two deformed nuclei, the β_{61} simply reinforces the effect of β_{41} or $\beta_{31} + \beta_{41}$. We have presented here the case of $\beta_{62} = 0$, but the same is found to be true for nonzero β_{62} .

Finally, we studied the effect of adding the still higher deformation β_8 . Since not much information is available about its magnitude, we consider it only as a variable, having both the negative and the positive values. Figure 9 shows the results of our calculation for the two cases of large, positive β_4 [Fig. 9(a)] and negative β_4 [Fig. 9(b); the same as for small, positive β_4]. The nuclei are so chosen that the addition of β_6 reinforces (inversely) the effect of β_4 , i.e., negative β_6 for large positive

β_4 and vice versa. Thus, we have here the cases of nec and ec for $\beta_6 = 0$, respectively, in Figs. 9(a) and 9(b). Interestingly, the addition of β_8 leaves nec as nec and ec as ec, which means again the reinforcing of the result of β_4 and/or $\beta_4 + \beta_6$. The same holds good for collisions involving deformed + deformed nuclei.

IV. SUMMARY

In this article, we have extended our earlier study [5] to include the effects of the higher multipole deformations β_6 and β_8 , as well as the octupole deformation β_3 , on the distribution of barriers in orientation degrees of freedom. In particular, we have been interested in the angle(s) of orientation for a most compact configuration of the heavy ions in a hot fusion reaction. This means a configuration with the highest barrier and/or the smallest interaction radius. Such a study is taken up for the first time and we have used here the fragmentation theory generalized for deformed and oriented nuclei within the nuclear proximity potential.

The results of our study are summarized in Table I. This involves the reactions with one spherical and one deformed nuclei or both deformed nuclei. We notice in Table I that the inclusion of the β_3 deformation, wherever available, is very important, along with the β_4 deformation, because it changes the nec configuration due to β_4 to ec, and vice versa. Next, though the inclusion of β_6 leaves the deformed-plus-deformed configuration unchanged, it is very important for spherical + deformed collisions. In this case, for $\beta_3 = 0$ the addition of β_6 reinforces the result of β_4 , but with an opposite sign. Whereas for negative β_3 the inclusion of β_6 results in an ec for its positive and small negative values and nec for its very small negative values, for positive β_3 it results in a nec configuration for all β_6 values. However, the inclusion of β_8 leaves not only the deformed + deformed but also the spherical + deformed configurations unchanged. Thus, the effective barrier or the angle(s) of compactness is found sensitive to the various multipoles of the nuclear shape and the inclusion of higher multipoles to quadrupole deformation is important at least up to β_6 for spherical-plus-deformed systems and up to β_4 for deformed-plus-deformed systems.

ACKNOWLEDGMENTS

This work is supported in parts by the Deutsche Forschungsgemeinschaft (DFG), the Alexander von Humboldt-Stiftung (AvH), the Department of Science and Technology (DST), the Government of India, and the Council of Scientific and Industrial Research (CSIR), India. R.K.G. thanks the DFG for a Mercator Guest Professorship, and Q.L. and S.K.P. thank the AvH for financial support.

[1] Yu. Ts. Oganessian, V. K. Utyonkov, Yu. V. Lobanov, F. Sh. Abdullin, A. N. Polyakov, I. V. Shirokovsky, Yu. S. Tsyganov, G. G. Gulbekian, S. L. Bogomolov, B. N. Gikal, A. N. Mezentsev, S. Iliev, V. G. Subbotin, A. M. Sukhov, A. A. Voinov,

G. V. Buklanov, K. Subotic, V. I. Zagrebaev, M. G. Itkis, J. B. Patin, K. J. Moody, J. F. Wild, M. A. Stoyer, N. J. Stoyer, D. A. Shaughnessy, J. M. Kenneally, and R. W. Loughheed, Phys. Rev. C **69**, 054607 (2004).

- [2] Yu. Ts. Oganessian, V. K. Utyonkov, Yu. V. Lobanov, F. Sh. Abdullin, A. N. Polyakov, I. V. Shirokovsky, Yu. S. Tsyganov, G. G. Gulbekian, S. L. Bogomolov, B. N. Gikal, A. N. Mezentsev, S. Iliev, V. G. Subbotin, A. M. Sukhov, A. A. Voinov, G. V. Buklanov, K. Subotic, V. I. Zagrebaev, M. G. Itkis, J. B. Patin, K. J. Moody, J. F. Wild, M. A. Stoyer, N. J. Stoyer, D. A. Shaughnessy, J. M. Kenneally, P. A. Wilk, R. W. Loughheed, R. I. Il'kaev, and S. P. Vesnovskii, *Phys. Rev. C* **70**, 064609 (2004).
- [3] R. K. Gupta, M. Balasubramaniam, R. Kumar, N. Singh, M. Manhas, and W. Greiner, *J. Phys. G: Nucl. Part. Phys.* **31**, 631 (2005).
- [4] R. K. Gupta, M. Manhas, G. Münzenberg, and W. Greiner, *Phys. Rev. C* **72**, 014607 (2005).
- [5] R. K. Gupta, M. Manhas, and W. Greiner, *Phys. Rev. C* **73**, 054307 (2006).
- [6] R. K. Gupta, N. Singh, and M. Manhas, *Phys. Rev. C* **70**, 034608 (2004).
- [7] M. Manhas and R. K. Gupta, *Phys. Rev. C* **72**, 024606 (2005).
- [8] P. Möller, J. R. Nix, W. D. Myers, and W. J. Swiatecki, *At. Data Nucl. Data Tables* **59**, 185 (1995).
- [9] A. Sobiczewski, Z. Patyk, S. Cwiok, and P. Rozmej, *Nucl. Phys. A* **485**, 16 (1988).